Cationic Terpolymerization of Vinyl Ethers, Oxetane, and Ketones via Concurrent Vinyl-Addition, Ring-Opening, and Carbonyl-Addition Mechanisms: Multiblock Polymer Synthesis and Mechanistic Investigation

Arihiro Kanazawa and Sadahito Aoshima**

Department of Macromolecular Science, Graduate School of Science, Osaka University, Toyonaka, Osaka 560-0043, Japan

kanazawaa11@chem.sci.osaka-u.ac.jp, aoshima@chem.sci.osaka-u.ac.jp

Abstract

Cationic terpolymerization of an alkyl vinyl ether (VE) with oxetane and methyl ethyl ketone (MEK) proceeded via concurrent vinyl-addition, ring-opening, and carbonyl-addition mechanisms. Highly selective crossover reactions occurred in a one-way cycle, resulting in the generation of multiblock polymers with constitutional repeating units comprising a poly(VE) block, a polyoxetane block, and a single MEK unit. The ketone efficiently functioned as a non-homopolymerizable monomer, which reacted with the oxetane-derived oxonium ion to generate an alkoxy group-adjacent carbocation, or an oxocarbenium ion. Furthermore, the resulting carbocation allowed to react with only VEs. The polymerization, which was induced with an initiating system of $Ph_3C^+PF_6^-$, 2,6-di-*tert*-butylpyridine, and 1,4-dioxane, was partly mediated by long-lived propagating species. NMR analysis of the chain end structures revealed that mono- and difluorophosphate moieties generated via the hydrolysis of PF_6^- were partially responsible for the generation of these long-lived species.

Introduction

The polymerization of different types of monomers has potential for generating polymers with novel properties, unique architectures, or unprecedented monomer sequences. To generate these polymers efficiently, crossover reactions must proceed between different types of propagating species and monomers. Because of the difficulty associated with employing these crossover reactions, polymerizations of different types of monomers have been limited to several examples, such as zwitterionic polymerization,[1,2] vinyl-addition and ring-opening polymerization,[3−10] and interconvertible radical and cationic polymerization.[11] The difficulty in crossover propagation reactions, however, can be harnessed as a strategy

for synthesizing sequence-controlled polymers. Indeed, the ring-opening terpolymerization of ethylene oxide, maleic anhydride, and tetrahydrofuran[12] and the zwitterionic terpolymerization of ethylene phenylphosphonite, a vinyl monomer with an electron-withdrawing group, and carbon dioxide[13] successfully yielded ABC-type alternating terpolymers because of the absence of homopropagation reactions and the selectivity of the crossover propagation reactions. Our group has also recently reported the cationic terpolymerization of vinyl ether (VE), cyclohexane oxide (CHO), and methyl ethyl ketone (MEK) via a one-way cycle of crossover propagation reactions.[14]

Each monomer preferentially undergoing homo- and crossover propagation reactions without causing side reactions is a requisite for polymerizing different types of monomers. Oxetane, a four-membered cyclic ether with a relatively high ring strain, is a suitable candidate for copolymerization with different types of monomers because the cationic homopolymerization of oxetane has a relatively low frequency of side reactions, such as cyclic oligomerizations. Since the first report[15,16] of polymerizing oxetane using BF_3 as a catalyst, several initiating systems have been reported to induce the cationic polymerization of oxetane[17−20]. In particular, the polymerization with the initiating system consisting of an oxonium ion and a hexafluoroantimonate counteranion proceeded in a controlled/living manner via the generation of long-lived species.[21]

The copolymerization of oxetane with a vinyl monomer via cationic vinyl-addition and ring-opening mechanisms is most likely difficult because the crossover reaction from the oxetane-derived oxonium ion to the vinyl monomer does not occur due to the negligible generation of an unstable, primary carbocation via ring opening. The use of a ketone, however, is expected to enable the terpolymerization of a vinyl monomer with oxetane in a manner similar to the terpolymerization of VE, CHO, and MEK.[14] Specifically, a ketone potentially reacts with an oxetane-derived oxonium ion and generates an alkoxy group-adjacent carbocation, or an oxocarbenium ion, which subsequently reacts with a VE monomer. This type of polymerization will also be efficient for synthesizing polymers with controlled sequences because of the occurrence of selective crossover reactions between specific monomers. In particular, ABC-type alternating terpolymers is obtained when homopropagation reactions are completely suppressed. Furthermore, multiblock polymers, which are often synthesized by multistep and complicated procedures,[22−24] can be generated in one step when polymerization reaction involves both efficient homopropagation reactions and several rounds of crossover reactions per chain.

In this study, we examined the cationic terpolymerization of VE, oxetane, and MEK via concurrent vinyl-addition, ring-opening, and carbonyl-addition mechanisms. An initiating system consisting of a trityl initiator with a weakly coordinating counteranion, 2,6-di-*tert*-butylpyridine (DTBP), and 1,4-dioxane was designed (Scheme 1) partly based on the initiating system for the controlled/living cationic homopolymerization of oxetane.[21] DTBP was used as a proton trap reagent,[25−27] although initiation reaction from protons was found to occur even in the presence of DTBP. 1,4-Dioxane was used as a weak Lewis base that stabilizes propagating species.[21,28,29] Accordingly, the polymerization proceeded in a one-way cycle of

crossover propagation reactions to yield polymers with multiblock sequences. In the latter part of this paper, the polymerization mechanisms were investigated in detail through NMR analysis of the chain end structures. Direct initiation reaction from the trityl initiator partly occurred, whereas many polymer chains had α-ends derived from protons that were generated via the reaction of the trityl initiator and protic impurities. In addition, the generation of mono- and difluorophosphate species via the degradation of PF_6^- was found to partly contribute to the generation of long-lived species (the word "long-lived species" is used for describing the species that keeps reactivity as a propagating species for sufficient time for even propagation of all the polymer chains and incorporates a quencher fragment such as alkoxy or phenoxy groups of alcohol or sodium phenoxide quenchers, respectively) in the terpolymerization.

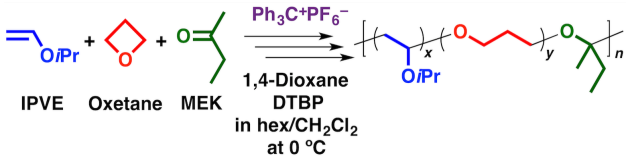

Scheme 1. Cationic terpolymerization of IPVE, oxetane, and MEK.

Experimental Section

Materials. Isopropyl VE (IPVE; Wako, 97.0+%) and ethyl VE (EVE; TCI, >98.0%) were washed with 10% aqueous sodium hydroxide solution, followed by water, and then distilled twice from calcium hydride. Oxetane (TCI, >98.0%) and MEK (Wako; 99.0+%) were distilled twice from calcium hydride. 2,6-Di-*tert*-butylpyridine (DTBP; Sigma-Aldrich, >97%) was distilled twice from calcium hydride under reduced pressure. 1,4-Dioxane (Wako; >99.5%) was distilled from calcium hydride and then lithium aluminum hydride. Triphenylcarbenium hexafluorophosphate ($Ph_3C^+PF_6^-$; Sigma-Aldrich), triphenylcarbenium tetrafluoroborate ($Ph_3C^+BF_4^-$; TCI, >98.0%), triphenylcarbenium tetrakis(pentafluorophenyl)borate [$Ph_3C^+B(C_6F_5)_4^-$; TCI, >98.0%], 3-buten-1-ol (TCI, >98.0%), silver hexafluorophosphate ($AgPF_6$; Strem, 99%), and hydrogen chloride solution (1.0 M in diethyl ether; Sigma-Aldrich) were used as received. Sodium phenoxide (PhONa) was prepared by the reaction of phenol (Nacalai Tesque, 99.0%) with sodium (Nacalai Tesque, 99%) in 1,4-dioxane.[30] Dichloromethane (Wako; 99.0%) and hexane (Wako; >96.0%) were dried by passage through solvent purification columns (Glass Contour). Dichloromethane-d_2 (Euriso-top) was distilled from calcium hydride. Chemicals except for trityl initiators, $AgPF_6$, 3-buten-1-ol, PhONa, dichloromethane, and hexane were stored in brown ampules under dry nitrogen.

Polymerization Procedures. The following is a typical polymerization procedure. A glass tube equipped with a three-way stopcock was dried under dry nitrogen using a heat gun (Ishizaki; PJ-206A; blow temperature of ~450 °C). Dichloromethane, hexane, 1,4-dioxane, IPVE, oxetane, and MEK were added into the tube using dry syringes. To the solution (1.97 mL), a dichloromethane solution (0.23 mL) containing

Ph_3CPF_6 (40 mM), DTBP (50 mM), and 1,4-dioxane (2.0 M) was added at 0 °C to initiate the polymerization. After predetermined intervals, small aliquots were extracted from the reaction mixture using dry syringes and then added into an alcohol (methanol or 3-buten-1-ol) solution containing a small amount of an aqueous ammonia. The quenched mixtures were diluted with dichloromethane and washed with an aqueous sodium hydroxide solution and then water. The volatiles were removed under atmospheric pressure at room temperature to yield polymers. The monomer conversion values of IPVE and oxetane were determined by gas chromatography (GC; column packing material: PEG-20M-Uniport-HP, GL Science Inc.) using hexane as an internal standard. The monomer conversion value of MEK was determined from the ^{1}H NMR integral ratios of the polymers.

Acid Hydrolysis. The acid hydrolysis of the copolymers was conducted using 0.5 M HCl(aq) in 1,2-dichloromethane at room temperature for 1 h (sample: ~1 wt%). The quenched mixture was diluted with dichloromethane and washed with an aqueous sodium hydroxide solution and then water. The volatiles were removed under atmospheric pressure at room temperature.

Characterization. The polymers' molecular weight distributions (MWDs) were measured via gel permeation chromatography (GPC) in chloroform at 40 °C on polystyrene gel columns (TSKgel GMH_{HR}-M × 2 with an exclusion limit molecular weight = 4×10^6; bead size = 5 mm; column size = 7.8 mm i.d. × 300 mm; flow rate = 1.0 mL min^{-1}) connected to a Tosoh DP-8020 pump, a CO-8020 column oven, a UV-8020 ultraviolet detector, and an RI-8020 refractive-index detector. The number-average molecular weight (M_n) and the polydispersity ratio (weight-average molecular weight/number-average molecular weight [M_w/M_n]) were calculated from the chromatographs based on 16 polystyrene standards (Tosoh; M_n = 577–1.09×10^6, $M_w/M_n \leq 1.1$). NMR spectra were recorded on JEOL JNM-ECA 500 (500.16 MHz for ^{1}H and 125.77 MHz for ^{13}C) or JEOL JNM-ECS 400 (376.17 MHz for ^{19}F and 161.83 MHz for ^{31}P) spectrometers. Hexafluorobenzene (–164.9 ppm) and phosphoric acid (0.00 ppm) were used as external standards for ^{19}F and ^{31}P NMR, respectively. Electrospray ionization mass spectrometry (ESI-MS) data were recorded on an LTQ Orbitrap XL (Thermo Scientific) spectrometer. Polymer solutions in dichloromethane/methanol (1/1 v/v) were used for ESI-MS analysis.

Results and Discussion

Cationic Terpolymerization of VE, Oxetane, and MEK

First, IPVE and oxetane were copolymerized using $Ph_3C^+PF_6^-$ as the initiator in the presence of DTBP and 1,4-dioxane in hexane/dichloromethane (8/2 v/v) at 0 °C. Both IPVE and oxetane were consumed to yield a polymer (entry 11 in Table 1). Analysis of the product by ^{1}H NMR and acid hydrolysis (Figure S1 in the Supporting Information), however, suggested that crossover propagation reactions had occurred from IPVE to oxetane (the upper reaction in Scheme 2A) but not from oxetane to IPVE (the upper reaction in

Scheme 2B). Thus, the product was mainly composed of diblock chains. The negligible crossover reaction from oxetane to IPVE is ascribed to the oxetane-derived oxonium ion neither reacting with a vinyl monomer nor generating a carbocation via the ring-opening reaction because of the instability of the primary carbocation.

Table 1. Cationic Terpolymerization of IPVE, Oxetane (Oxt), and MEK; Copolymerization of Two of the Three Monomers; and Homopolymerization.[a]

Entry	$[VE]_0$	$[Oxt]_0$	$[MEK]_0$	Time	VE conv. (%)[b]	Oxt conv. (%)[b]	MEK conv. (%)[c]	$M_n \times 10^{-3}$ (calcd)	$M_n \times 10^{-3}$ (exp)[d]	M_w/M_n[d]	Average unit numbers per block[e]		
											VE	Oxt	MEK
1	0.80	0.81	2.0	0.8 h	17	20	0.3	5.3	7.8	2.27	19	21	0.76
2				21 h	87	67	1.2	23.2	17.6	1.82	24	18	0.82
3	0.80	0.40	2.0	0.8 h	23	9	0.1	4.5	6.5	2.34	45	10	0.80
4				9 h	75	34	0.5	14.9	12.2	1.89	46	12	0.79
5	0.80	1.6	2.0	1.5 h	2	7	0.1	2.0	6.0	2.45	5.6	34	0.79
6				5 h	29	57	0.8	18.3	21.6	2.03	11	42	0.71
7	0.80	0.81	0.40	2.5 h	7	32	1.4	5.0	13.3	3.13	20	46	0.98
8				24 h	54	75	2.2	18.2	30.2	2.19	39	49	0.71
9[f]	0.81	0.81	2.0	4 h	9	25	0.2	4.3	5.5	1.94	6.5	26	0.62
10[f]				24 h	51	76	1.4	16.7	12.0	1.94	12	17	0.77
11	0.80	0.81	–	24 h	20	79	–	12.7	49.4	2.45	41	122	–
12	–	0.81	2.0	192 h	–	12	0	1.4	1.7	2.34	–	–	–
13	0.80	–	2.0	20 min	80	–	0	11.5	9.2	2.37	–	–	–
14	0.80	–	–	9 min	93	–	–	16.1	6.1	3.03	–	–	–
15	–	0.81	–	144 h	–	3	–	–	–	–	–	–	–
16	–	–	2.0	120 h	–	–	0	–	–	–	–	–	–

[a] $[Ph_3C^+PF_6^-]_0$ = 4.0 mM, [DTBP] = 5.0 mM, [1,4-dioxane] = 1.0 M, in hexane/dichloromethane (8/2 v/v; entries 1–8, 11, and 16) or dichloromethane (with 6 vol% of hexane as an internal standard for GC; entries 9, 10, and 12–15) at 0 °C. [b] By GC. [c] By ^{1}H NMR. [d] By GPC (polystyrene calibration). [e] Estimated by ^{1}H NMR. The values correspond to the unit numbers per acetal. [f] EVE was used instead of IPVE.

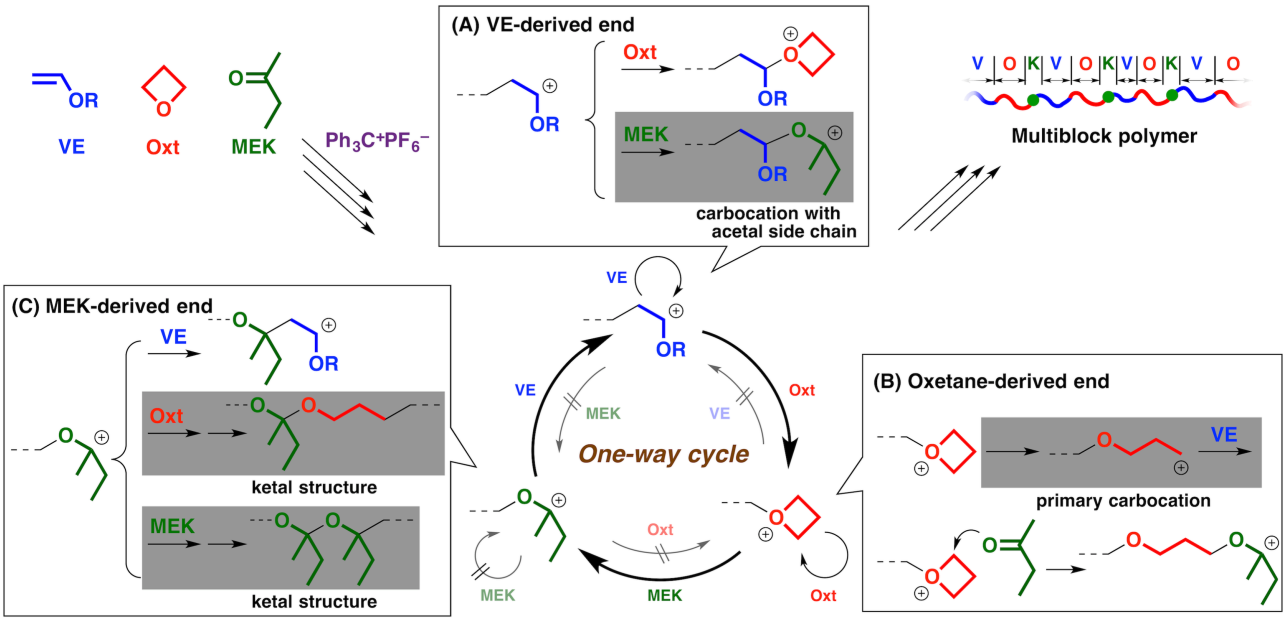

Scheme 2. Propagation reactions in the terpolymerization of VE, oxetane, and MEK. Reactions with gray shadow do not proceed due to the instability of the resulting cations or structures. Counteranions are omitted.

To enable polymerization via efficient crossover reactions, MEK was added as the third monomer to the polymerization of IPVE and oxetane. MEK was expected to react with the oxetane-derived oxonium ion by attacking the methylene carbon adjacent to the cationic oxygen atom (the lower reaction in Scheme 2B) in a manner similar to the terpolymerization of IPVE, CHO, and MEK.[14] As shown in Figure 1A, the terpolymerization smoothly proceeded to reach a relatively high conversion of VE and oxetane (entries 1 and 2 in Table 1). A small amount of MEK was also consumed, as confirmed by the ^{1}H NMR analysis of the products (Figure 2; explained in the next paragraph). The product polymers had unimodal MWDs, although the M_w/M_n values were relatively large. Notably, the M_n values of the polymers increased as the polymerization proceeded, indicating that long-lived species were partially generated during polymerization (black curves in Figure 1C). The M_n values determined by polystyrene-calibrated GPC were relatively consistent with the theoretical values calculated from the monomer conversion values (Figure 1B). The cause of the generation of long-lived species is discussed in the next section.

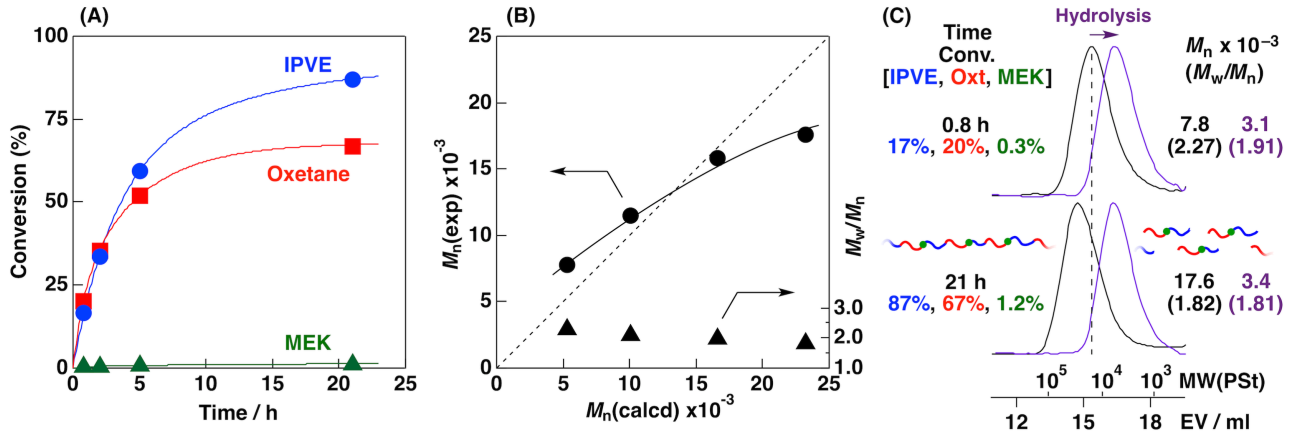

Figure 1. (A) Time–conversion plots for the terpolymerization of IPVE, oxetane (Oxt), and MEK, (B) M_n and M_w/M_n values, and (C) MWD curves (black: original polymers, purple: products obtained by acid hydrolysis) of the obtained polymers {$[IPVE]_0$ = 0.80 M, $[oxetane]_0$ = 0.81 M, $[MEK]_0$ = 2.0 M, $[Ph_3C^+PF_6^-]_0$ = 4.0 mM, [DTBP] = 5.0 mM, [1,4-dioxane] = 1.0 M, in hexane/dichloromethane (8/2 v/v) at 0 °C}.

^{1}H NMR analysis suggested that a polymer with a multiblock sequence was generated by terpolymerization via efficient crossover propagation reactions. In addition to peaks assigned to structures derived from IPVE, oxetane, and MEK, the spectrum (Figure 2A, entry 2 in Table 1) featured a peak at 4.6–4.7 ppm that was assigned to an acetal structure generated through the crossover reaction from the IPVE-derived propagating end to oxetane. According to the integral ratios of the acetal peak to the peaks of each monomer, the average IPVE, oxetane, and MEK units in each block were estimated to be 24, 18, and 0.82.[31] The relatively large unit numbers of IPVE and oxetane in each block most likely stemmed from the preference for homopropagation reactions over crossover reactions at the propagating ends derived from IPVE and oxetane unlike in the case of the terpolymerization of IPVE, CHO, and MEK.[14]

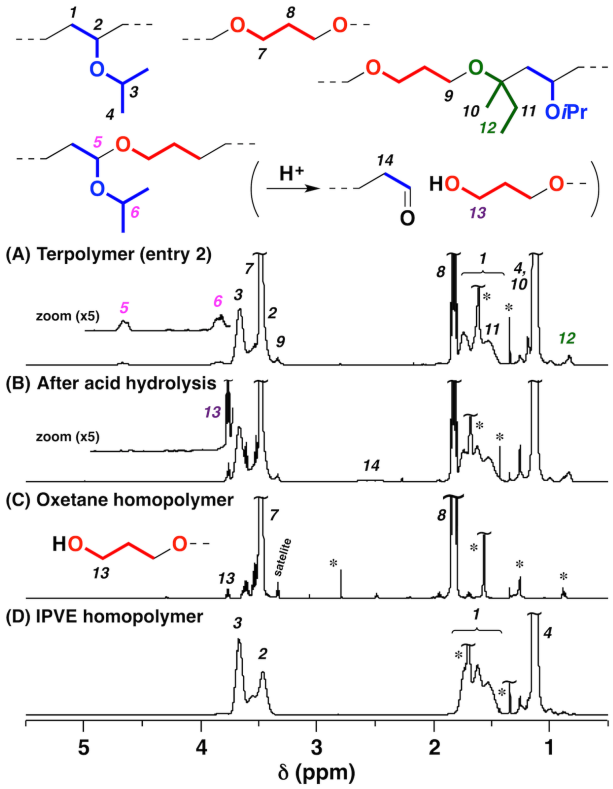

Figure 2. ^{1}H NMR spectra of (A) IPVE–oxetane–MEK terpolymer (entry 2 in Table 1), (B) its hydrolysis product, (C) oxetane homopolymer [produced at 30 °C under the same conditions to those for entry 15 in Table 1; M_n(GPC) = 19.8 × 10^3, M_w/M_n(GPC) = 2.04], and (D) IPVE homopolymer (entry 14) (in $CDCl_3$ at 30 °C; * water, DTBP, or vaseline).

The generation of a multiblock polymer was also confirmed by acid hydrolysis. The product polymer was degraded under acidic conditions via the cleavage of the acetal moieties in the main chain, affording a product with a unimodal MWD (purple curves in Figure 1C). Moreover, the hydrolysis products of the polymers with low and high monomer conversion values had similar M_n values, suggesting that in the terpolymerization of these monomers under the reaction conditions employed, the block lengths were similar irrespective of the monomer conversion. Furthermore, the block length of the terpolymers (entries 1 and 2 in Table 1) was consistent with that by ^{1}H NMR analysis of the polymers before acid hydrolysis (Figure 2A and 2B).

The polymerization results using one or two monomers indicated that all three monomers were indispensable for the efficient polymerization yielding multiblock polymers. The copolymerization of IPVE and oxetane resulted in the generation of a product mainly comprising diblock chains (entry 11 in Table 1), as described above. The reaction of IPVE and MEK produced an IPVE homopolymer (entry 13) because of the non-homopolymerizability of MEK (the lower reaction in Scheme 2C, entry 16) and the inefficient generation of carbocations with acetal side chain from the reaction between the VE-derived carbocation and MEK (the lower reaction in Scheme 2A). The reaction of oxetane and MEK also resulted in the generation of an oxetane homopolymer (entry 12), which arose from the instability of a ketal structure resulting from the

crossover reaction from MEK to oxetane (the middle reaction in Scheme 2C). In addition, the homopolymerization of IPVE proceeded (entry 14), whereas the homopolymerization of oxetane hardly occurred at 0 °C (entry 15).[32] This result suggests that the system of $Ph_3C^+PF_6^-$, DTBP, and 1,4-dioxane is not suited for initiating oxetane polymerization at 0 °C. This is in contrast to past examples of oxetane polymerization at lower temperature using other initiating systems[15−19] or $Ph_3C^+PF_6^-$ alone.[20]

These results demonstrated that the terpolymerization of IPVE, oxetane, and MEK proceeded via a one-way cycle of crossover propagation reactions in the direction of IPVE → oxetane, oxetane → MEK, and MEK → IPVE (Scheme 2). Multiblock polymers with constitutional repeating units comprising a poly(VE) block, a polyoxetane block, and a single MEK unit were obtained through several rounds of crossover reactions per chain (e.g. 4-5 rounds per chain for the lower polymer in Figure 1C). In particular, MEK efficiently functioned in the terpolymerization through a series of reactions, including attacking the oxetane-derived oxonium ion (the left side of the lower reaction in Scheme 2B), generating an alkoxy group-adjacent carbocation, or an oxocarbenium ion (the right side of the lower reaction in Scheme 2B), and subsequently reacting the resultant carbocation with an IPVE monomer (the upper reaction in Scheme 2C).

The average unit numbers of IPVE and oxetane in each block was dependent on the initial concentration of the monomers because of the resultant change in the frequency of homopropagation and crossover propagation reactions. The production of terpolymers with longer VE blocks and shorter oxetane blocks at lower concentrations of oxetane (entries 3 and 4 in Table 1) was caused by the decrease and increase in the frequencies of crossover reactions from VE to oxetane and from oxetane to MEK, respectively. By contrast, the terpolymers obtained at a higher concentration of oxetane had shorter VE and longer oxetane blocks (entries 5 and 6). Additionally, decreasing the MEK concentration resulted in products with longer oxetane blocks (entries 7 and 8). The use of EVE, a less reactive VE than IPVE, yielded terpolymers with shorter VE blocks because of the increase in the frequency of crossover reactions from VE to oxetane (entries 9 and 10; Figure S2).

The results of terpolymerization reactions in the absence of DTBP or 1,4-dioxane suggested that DTBP is needed for the generation of polymers with high MWs, whereas 1,4-dioxane marginally affects the polymerization. The reaction without DTBP provided polymers with much lower MWs than those obtained in the presence of DTBP (Figure S3), indicating that DTBP partly suppressed undesired reactions, such as chain-transfer reactions, as a proton trap reagent (although protons, in conjunction with the trityl initiator, appeared to serve as an initiating species, even in the presence of DTBP; vide infra). The polymerization in the absence of 1,4-dioxane proceeded in a manner similar to the reaction in its presence and yielded similar polymers (Figure S4). Interestingly, a small amount of 1,4-dioxane was incorporated into polymer chains, as demonstrated in the next section, indicating that 1,4-dioxane functioned as a weak Lewis base and interacted with the propagating species. However, the effect of 1,4-dioxane on the generation of long-lived species appears to be small in the present system. This is potentially because oxetane, which exhibits a stronger Lewis basicity than 1,4-dioxane,[33,34] also functioned not only as a monomer but also as an important

ingredient that interacts with propagating species.

Elucidation of Polymerization Mechanisms via Chain End Analysis

The polymerization mechanisms were investigated with particular focus on the cause of the generation of long-lived species. Accordingly, NMR analysis of the chain end structures was conducted as described below.

Analysis of α-ends

To investigate the initiation reaction, terpolymerization was conducted at different concentrations of $Ph_3C^+PF_6^-$. The reactions proceeded smoothly, yielding polymers with unimodal distributions in all cases. The M_n values of the products obviously depended on the amount of $Ph_3C^+PF_6^-$ (Figure 3), indicating that the polymer chains were generated from a reaction involving trityl cations.

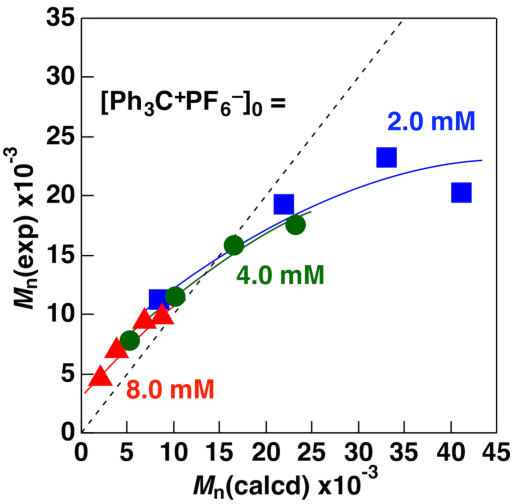

Figure 3. M_n values of IPVE–oxetane–MEK terpolymers obtained using different concentrations of $Ph_3C^+PF_6^-$ {$[IPVE]_0$ = 0.80 M, $[oxetane]_0$ = 0.81 M, $[MEK]_0$ = 2.0 M, $[Ph_3C^+PF_6^-]_0$ = 2.0 (blue squares), 4.0 (green circles; the same data to those shown in Figure 1), or 8.0 (red triangles) mM, [DTBP] = 2.5, 5.0, or 10 mM (1.25 times the amount of $Ph_3C^+PF_6^-$), [1,4-dioxane] = 1.0 M, in hexane/dichloromethane [8/2 (blue and green) or 7/3 (red) v/v] at 0 °C}.

Chain end analysis by ^1H NMR (Figure S5), however, revealed that in most cases, less than 10–20% of the polymer chains had incorporated trityl moieties (Figure 4). Instead, most of the polymers had α-ends generated by the reaction between a proton and a VE monomer. Although the exact source remains unclear, protons were likely generated from the reaction of the trityl initiator and protic species such as adventitious water.[35] The relatively large M_w/M_n values (approximately 2) of the terpolymers are likely derived from the slow and uneven initiation reaction via such a process. In addition, peaks assigned to the

initiator fragments, such as Ph_3COH (3.0–3.1 ppm) and Ph_3CH (5.55 ppm), were observed in ^1H NMR spectra of the product polymers. These species also appear to be related to the indirect initiation reaction of the trityl initiator.[35,36]

The occurrence of initiation reactions from protons even in the presence of DTBP is unusual in terms of general recognition concerning the role of DTBP as a proton trap reagent;[25–27] however, initiation reactions from protons are not always suppressed in the presence of DTBP, which was demonstrated by the experimental results of IPVE polymerization using HCl, $AgPF_6$, and DTBP. A protic acid having a PF_6^- counteranion (tentatively represented as "$H^+PF_6^-$") was generated in situ by the reaction of HCl and $AgPF_6$ ($[HCl]_0/[AgPF_6]_0$ = 5/4) in dichloromethane, accompanied by the formation of AgCl precipitate.[37–40] Subsequently, the supernatant solution of this mixture containing the protic acid was added to an DTBP solution in dichloromethane. Interestingly, polymerization of IPVE proceeded in the solution containing this protic acid (4.0 mM) and an excess amount of DTBP (10 or 20 mM; Table 2). The result indicates that protons, which had been most likely trapped by DTBP, were liberated and subsequently initiated the polymerization reaction. Moreover, the polymerization rates were much lower than that in the absence of DTBP and the M_n values of the products were not high, indicating that polymerization started from a part of protons and proceeded partly via chain-transfer reactions (indeed, the structure resulting from β-proton elimination reactions was confirmed by ^1H NMR analysis). A very weak basicity of the counteranion (PF_6^-) of the proton–DTBP adduct would affect the liberation of the proton because initiation reactions were inefficient using HCl alone (4.0 mM) as a protic acid in the presence of DTBP (20 mM; Figure S6B). A high reactivity of a VE, which is a cationically polymerizable monomer that exhibits a higher reactivity than styrene derivatives and isobutylene, may also be responsible for the initiation reactions from protons in the presence of DTBP. Indeed, oxetane homopolymerization was not initiated using $Ph_3C^+PF_6^-$ in the presence of DTBP at 0 °C as demonstrated in the previous section (entry 15 in Table 1).

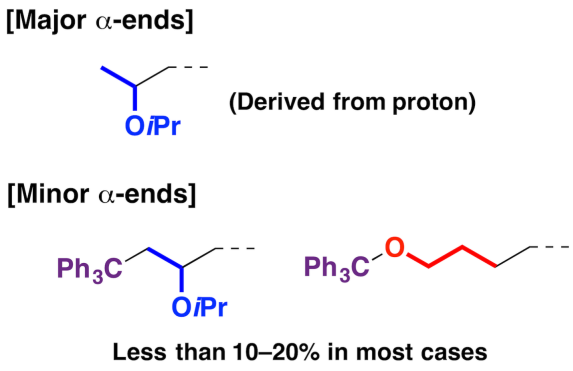

Figure 4. Structures of the α-ends (see Figure S5 for ^1H NMR spectra).

Table 2. Cationic Polymerization of IPVE Using Protic Acid with PF_6^- Counteranion in the Presence of DTBP.[a]

[Generated protic acid]$_0$ (mM)[b]	[DTBP] (mM)	Time	Conv (%)[c]	$M_n \times 10^{-3}$ [d]	M_w/M_n [d]
4.0	0	10 s	99	11.7	5.56
4.0	10	3 h	89	6.1	2.31
4.0	20	6 h	88	4.4	1.95

[a] $[IPVE]_0$ = 0.80 M, [1,4-dioxane] = 1.0 M, $[Et_2O]$ = 0.05 M, in dichloromethane at 0 ºC. See Figure S6A for time–conversion plots. [b] Protic acid with PF_6^- counteranion was generated by the reaction of HCl (50 mM) and $AgPF_6$ (40 mM). The supernatant solution of this mixture was used for polymerization. [c] By GC. [d] By GPC (polystyrene calibration).

Analysis of ω-ends

The structures of the long-lived propagating species were investigated through chain end analysis of polymers. 3-Buten-1-ol was used as a quencher because the olefin moiety is useful for quantitative analysis of chain ends by ^{1}H NMR. Figure 5 shows ^{1}H NMR spectra of (A) the IPVE–oxetane-MEK terpolymer, (B) the IPVE homopolymer, and (C) the oxetane homopolymer. To produce polymers with low MWs, these polymers were prepared using larger amounts of $Ph_3C^+PF_6^-$ (12 mM) than those used for the experiments conducted above. Peaks 17 and 18 were assigned to the alcohol quencher-derived olefin structure, which was incorporated into the acetal chain end through the reaction of the VE-derived propagating chain end and the alcohol. This peak disappeared after acid hydrolysis of the terpolymer (Figure 5A-1) because of the degradation of the acetal structure. The structure generated from the oxetane-derived propagating end (peaks 22 and 23; vide infra) was also identified as an olefin unit derived from 3-buten-1-ol.

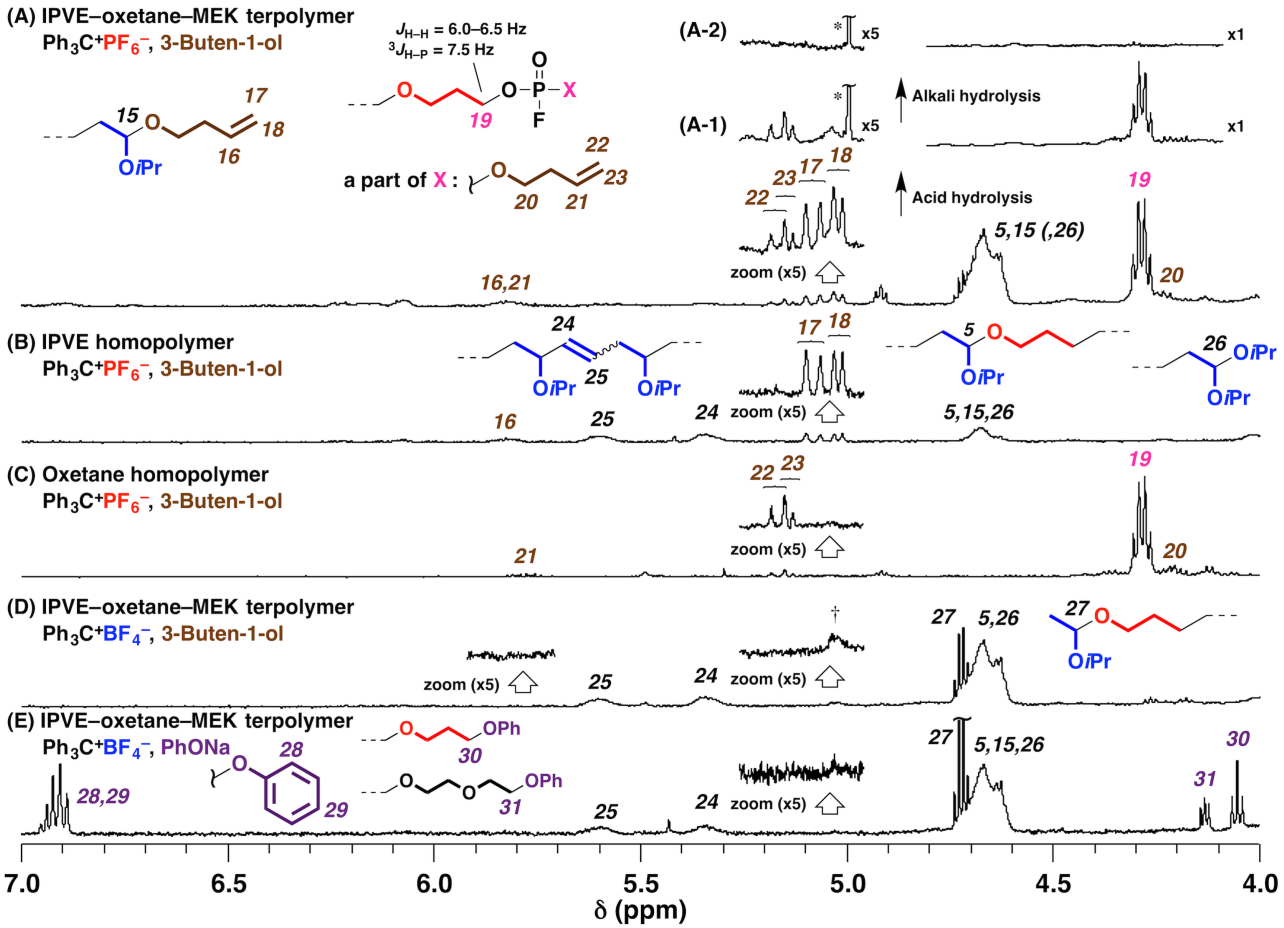

Figure 5. ^{1}H NMR spectra of polymers obtained using larger amounts (12 mM) of trityl initiators than those for the polymers listed in Table 1. 3-Buten-1-ol or PhONa was used as a quencher. Low-MW portions were removed by preparative GPC. Polymerizations were quenched at low monomer conversion to obtain low-MW products {polymerization conditions: $[IPVE]_0$ = 0.80 M (for A, B, D, and E), $[oxetane]_0$ = 0.80 M (for A, C, D, and E), $[MEK]_0$ = 0.80 M (for A, D, and E), $[Ph_3C^+PF_6^-$ or $Ph_3C^+BF_4^-]_0$ = 12 mM, [DTBP] = 15 mM, in hexane/dichloromethane (5/2 v/v) (for A) or dichloromethane (with 5 or 6 wt% of hexane) for (B–E), at 0 °C; GPC data analyzed after separation by preparative GPC: (A) M_n(GPC) = 5.0 × 10^3, M_w/M_n(GPC) = 1.53, (B) M_n(GPC) = 8.7 × 10^3, M_w/M_n(GPC) = 1.52, (C) M_n(GPC) = 14.4 × 10^3, M_w/M_n(GPC) = 3.74, (D) M_n(GPC) = 8.0 × 10^3, M_w/M_n(GPC) = 1.80, (E) M_n(GPC) = 8.8 × 10^3, M_w/M_n(GPC) = 1.50}. † 3-Buten-1-ol, used as a quencher, was slightly incorporated to the product obtained using $Ph_3C^+BF_4^-$ because the area ratio of the peak at 5.8ppm was smaller than the value expected from the area ratio of the peak at 5.0–5.1ppm.

Chain end analysis also indicated that mono- and difluorophosphate structures were partly generated at the propagating end. The doublet of triplets peak at 4.29 ppm in the ^{1}H NMR spectrum of the terpolymer was assigned to the methylene protons of oxetane-derived units bonded to a fluorophosphate (peak 19 in Figure 5A). This assignment was confirmed via ^{1}H, ^{13}C, ^{1}H-^{1}H COSY, ^{1}H-^{13}C HSQC, ^{1}H-^{13}C HMBC, ^{31}P and ^{19}F NMR analyses of an EVE-oxetane-MEK terpolymer, as shown in the Supporting Information (Figures S7–S12).[41−43] The high-resolution ESI-MS spectrum of the oxetane homopolymer also

exhibited chains with monofluorophosphate moieties (Figure S13). The mono- and difluorophosphate structures were most likely generated from the hydrolysis of PF_6^- by adventitious water (Scheme 3).[42—46] Indeed, the ^{31}P and ^{19}F NMR spectra of the mixture of $Ph_3C^+PF_6^-$, DTBP, and 1,4-dioxane in dichloromethane-d_2 had peaks ascribed to mono- and difluorophosphates (Figure S14). Although the detailed mechanism is unclear, these peaks being negligible in the spectrum of $Ph_3C^+PF_6^-$ alone suggested that DTBP and/or 1,4-dioxane promoted the hydrolysis reaction.

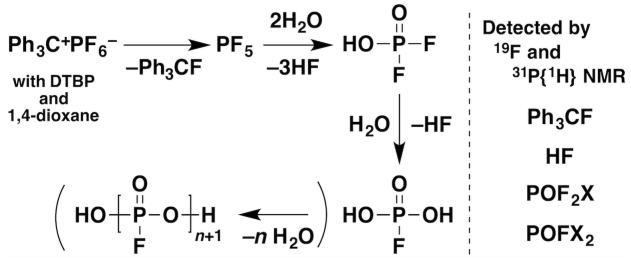

Scheme 3. Possible mechanisms (cf. references 42—46) of hydrolysis reactions of $Ph_3C^+PF_6^-$ into mono- and difluorophosphates by adventitious water in the presence of DTBP and 1,4-dioxane in dichloromethane. See Figure S14 for the ^{19}F and $^{31}P\{^1H\}$ NMR spectra.

The mono- and difluorophosphate species most likely functioned as reversible chain-transfer agents during the terpolymerization reaction, as observed in the case of the cationic polymerization of VEs using phosphates.[47] The reaction mechanisms concerning phosphates are shown in Scheme 4. Mono- and difluorophosphates generated via the hydrolysis of PF_6^- react with the propagating oxonium ion derived from oxetane, which generates a phosphate species bearing an oxetane-derived propagating chain (the upper reaction in Scheme 4). This phosphate-incorporated chain end also reacts with another oxonium ion to generate an intermediate cation, and then either of the two oxetane-derived chains are liberated via the attack of an oxetane monomer on the methylene carbon adjacent to the phosphate moiety (the lower reaction in Scheme 4). Phosphate generation and chain-transfer reactions also likely occur at the VE-derived chain ends. However, whether the chain-transfer reactions between different types of propagating species, such as the reaction between the VE-derived carbocation and the oxetane-derived phosphate species, occur is unclear. The results of the terpolymerization of IPVE, oxetane, and MEK and the homopolymerization of oxetane in the presence of $(EtO)_3PO$ (Figures S15 and S16) also supported the function of phosphates as reversible chain-transfer agents.

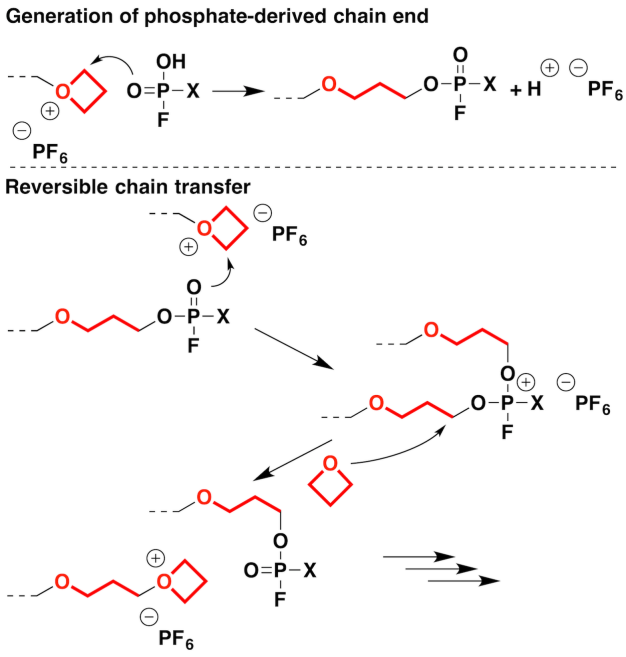

Scheme 4. Generation of phosphate-derived propagating chain ends and the propagation reaction via the reversible chain-transfer mechanism. VE- or MEK-derived propagating species potentially generate similar phosphate-derived ends (possible structures of X: F, OR, and OH).

The oxetane-derived monofluorophosphate end remained intact after quenching with an alcohol (species v in Scheme 5A), whereas the difluorophosphate structure was most likely converted into a monofluorophosphate through reaction with the alcohol (species vi and structure vi-OR'). The high-resolution ESI-MS spectrum of the oxetane homopolymer (Figure S13) had peaks ascribed to monofluorophosphate-incorporated chains, both with and without a quencher-derived alkoxy group. In addition, peaks 22 and 23 in the ^{1}H NMR spectrum (Figure 5) were assigned to the olefin moiety of a structure consisting of an oxetane chain, fluorophosphate moiety, and quencher-derived alkoxy group, a hypothesis which was also supported by the disappearance of peaks 22, 23, and 19 after alkali hydrolysis (Figure 5A-2). The calculated free energy of the hydrolysis reaction of a difluorophosphate into a monofluorophosphate is reported to be lower than that of a monofluorophosphate to a phosphate.[42]

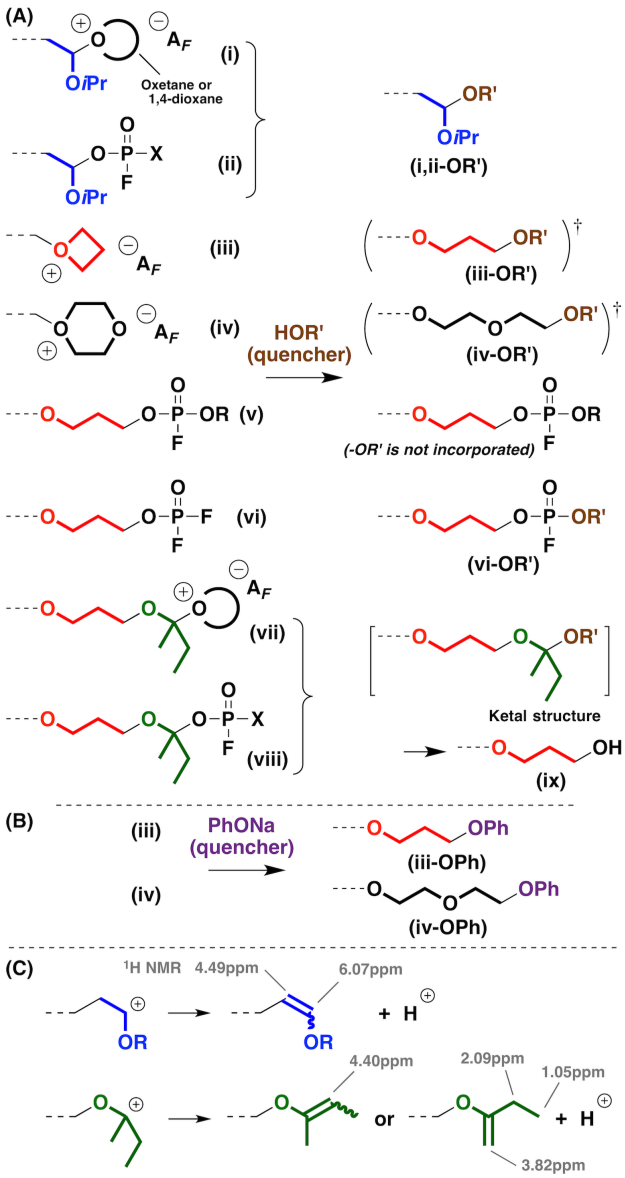

Scheme 5. (A) Possible propagating and dormant species. Structures generated after reaction with alcohol quencher are shown on the right side. (B) Structures generated when PhONa was used as a quencher (see Figure 5E for the ^{1}H NMR spectrum). (C) β-Proton elimination reactions that occurred at the VE- or MEK-derived carbocations (see Figure S20 for the ^{1}H NMR spectra). A_F^- stands for non- or weakly coordinating anions such as PF_6^-, BF_4^-, or $B(C_6F_5)_4^-$. † Structures iii-OR' and vi-OR' were not confirmed, whereas peaks whose *m*/*z* values corresponds to the mass values of structure vi-OR' were detected in the ESI-MS analysis of an oxetane homopolymer (Figure S13).

Polymerization results using $Ph_3C^+B(C_6F_5)_4^-$ or $Ph_3C^+BF_4^-$ as the initiator indicated that the mono- and difluorophosphate-derived chain ends are not always required for generating long-lived species, as multiblock polymers were successfully produced via reactions using these initiators instead of $Ph_3C^+PF_6^-$. Moreover, the M_n values of the products increased as the polymerization proceeded (Figure 6) in a manner similar to the case of polymerizations initiated by $Ph_3C^+PF_6^-$. The result suggests that the difference in coordination ability among $B(C_6F_5)_4^-$, a non-coordinating anion, and PF_6^- and BF_4^-, weakly coordinating

anions, slightly affected initiation, propagation, and side reactions in terpolymerization. However, the smaller M_n values of the products from $Ph_3C^+BF_4^-$ than those of the products from the other trityl initiators stemmed from the formation of non-negligible amounts of cyclic oligomers (Figure S17A).

Importantly, when used as a quencher, 3-buten-1-ol was negligibly incorporated into the chain ends of the terpolymer obtained using $Ph_3C^+BF_4^-$. This result indicates that the VE-derived propagating chain ends (species i in Scheme 5A) were mainly absent and that the alcohol did not react efficiently with the oxetane-derived ends (species iii), the latter of which was confirmed by quenching the polymerization with PhONa. The product obtained using PhONa, which was reported to be an effective quencher of oxetane homopolymerization,[17] had peaks corresponding to the phenoxy group at 6.88–6.96 ppm. The triplet peak at 4.06 ppm was assigned to the oxetane-derived methylene group adjacent to the phenoxy group (structure iii-OPh in Scheme 5B),[48,49] indicating that the oxonium ion generated from oxetane functioned as a long-lived species. In addition, the spectrum had a peak at 4.13 ppm, which most likely corresponded to the 1,4-dioxane-derived methylene peak adjacent to the phenoxy group (structure iv-OPh in Scheme 5B).[48,50] 1,4-Dioxane appeared to function as a weak Lewis base, forming an oxonium ion by reacting with the oxetane-derived propagating species (species iv) in a manner similar to the oxetane homopolymerization reported in a past study.[21] In addition, the incorporation of 1,4-dioxane into the polymer chains was confirmed by ESI-MS analysis of the homopolymer (Figure S13).

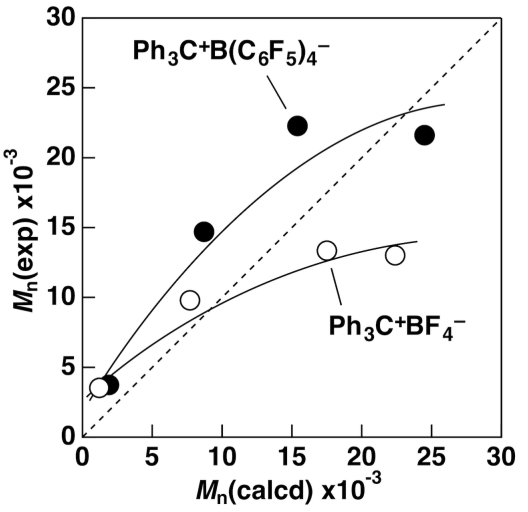

Figure 6. M_n values of the IPVE–oxetane–MEK terpolymers obtained using $Ph_3C^+B(C_6F_5)_4^-$ (filled) or $Ph_3C^+BF_4^-$ (open) {$[IPVE]_0$ = 0.80 M, $[oxetane]_0$ = 0.81 M, $[MEK]_0$ = 2.0 M, $[Ph_3C^+B(C_6F_5)_4^-$ or $Ph_3C^+BF_4^-]_0$ = 4.0 mM, [DTBP] = 5.0 mM, [1,4-dioxane] = 1.0 M, in hexane/dichloromethane (8/2 v/v) at 0 ºC. See Figure S17 for the time–conversion plots of polymerization reactions and the MWD curves of the obtained polymers and hydrolysis products}.

The structures of possible propagating species that are present during terpolymerization and/or that function as dormant species (Scheme 5A) are discussed based on the chain end analysis described above.

The estimated ratios of detectable ω-ends are summarized in Table 3. The VE-derived propagation ends are considered to be oxetane- or 1,4-dioxane-attached cationic species (i) or fluorophosphate species (ii). The minor incorporation of the alcohol quencher in the reaction using $Ph_3C^+BF_4^-$ (Figure 5D) suggests that species i is largely absent, whereas species ii is generated in the reaction using $Ph_3C^+PF_6^-$. The oxetane-derived oxonium ion (iii) most likely functions as a long-lived propagating species, as confirmed by the incorporation of the phenoxy group when PhONa was used as the quencher (Figure 5E). The oxonium ion derived from 1,4-dioxane (iv) also likely functions as a dormant (and propagating) species. Importantly, mono- and difluorophosphate-attached chains (ii, v and vi) were major propagating species in the polymerization using $Ph_3C^+PF_6^-$ (entries I, II, and III in Table 3). In addition, the peaks for phenoxy groups attached to the methylene groups derived from oxetane or 1,4-dioxane in the polymer obtained using $Ph_3C^+PF_6^-$ were smaller (Figure S18) than those in the product obtained by $Ph_3C^+BF_4^-$ (entries III and IV in Table 3), indicating that the concentration of the propagating oxonium ions are dependent on the presence of mono- and difluorophosphates. The structure resulting from the reactions of the MEK-derived species (vii and viii) with an alcohol quencher is a ketal structure, which is unstable and is easily decomposed into the oxetane-derived hydroxy end (structure ix). The generation of a hydroxy group was confirmed by reaction with propionyl chloride (Figure S19); however, the hydroxy group can be generated by other reactions, including acid hydrolysis of the acetal structure in the main chain and degradation of the enol ether structures resulting from β-proton elimination (vide infra). Thus, whether MEK-derived species (vii and viii) were mainly present is unclear.

Table 3. The ratios of detectable ω-ends estimated by ^{1}H NMR analysis[a]

Entry[b]	Initiator, quencher	VE conv (%)	Oxt conv (%)	Ratio of ω-ends (%)			
				VE (i,ii)	Oxetane (iii)	1,4-Dioxane (iv)	Oxetane-attached phosphates (v, vi)
I	$Ph_3C^+PF_6^-$ 12 mM, 3-buten-1-ol	28	25	9	n.d.[c]	n.d.[c]	46
II	$Ph_3C^+PF_6^-$ 4.0 mM, 3-buten-1-ol	34	36	8	n.d.[c]	n.d.[c]	13
III	$Ph_3C^+PF_6^-$ 12 mM, PhONa	25	27	4	2	1	44
IV	$Ph_3C^+BF_4^-$ 12 mM, PhONa	25	22	(<2)[d]	10	7	–

[a] The values were roughly estimated from the integral ratios in the ^{1}H NMR spectra and the M_n value determined by GPC using polystyrene calibration. Other possible chain ends, which were not estimated in the analysis, include enol ether structures derived from β-proton elimination reaction and hydroxy groups derived from oxetane (the presence was confirmed; see text). Polymers were analyzed after the removal of low-MW portions by preparative GPC (except for entry II). See Scheme 5A for species i—vi. [b] Entry I: Figure 5A, entry II: A polymer that was obtained under the same conditions to those of entries 1 and 2 in Table 1 {M_n(GPC) = 11.5 × 10^3, M_w/M_n= 2.09}, entry III: Figure S18, entry IV: Figure 5E. [c] Not determined because an alcohol quencher is likely inefficient for the reactions with these propagating species. [d] The difference of the integral ratios of the phenoxy peaks (6.88–6.96ppm) and the triplet peaks at 4.06 ppm and 4.13 ppm was attributed to this value.

The nature of the oxetane-derived oxonium ion (species iii) is primarily responsible for the generation of long-lived species in the terpolymerization of VE, oxetane, and MEK. Negligible side reactions, except for cyclic oligomerization, occur at the oxetane-derived propagating end, which is consistent with the previous results obtained for oxetane homopolymerization.[17−21] The mono- and difluorophosphate species (v and vi) also contribute to the polymerization mediated by long-lived species. By contrast, β-proton elimination reactions occurred at the propagating ends derived from VE and MEK. The ^{1}H NMR spectra (Figure S20) contained peaks assigned to enol ether structures generated via β-proton elimination reactions at the VE- or MEK-derived propagating chain ends (Scheme 5C). These enol ether structures are highly susceptible to acid and thus were degraded into an aldehyde end or an oxetane-derived primary hydroxy end via acid hydrolysis. Therefore, the enol ether structures completely disappeared after separation via preparative GPC because of degradation induced by adventitious acid present in the chloroform eluent, which is a major reason for the difficulty associated with conducting quantitative analyses of chain end structures (detectable ω-ends are summarized in Table 3). Additionally, the smaller M_n values of the products obtained at the later stage of polymerization compared to the theoretical values indicate the occurrence of chain-transfer reactions because of the protons generated via the β-proton elimination reactions, even in the presence of DTBP, a proton trap reagent. Termination reaction also appeared to occur, which is deduced from the time–conversion curves (Figure 1A). Both the IPVE and oxetane conversion values appear to reach plateau at the later stage of the polymerization. The partial absence of reinitiation reactions from the protons liberated via the β-proton elimination reactions is likely responsible for the termination reaction.

Conclusion

In conclusion, the cationic terpolymerization of IPVE, oxetane, and MEK in a one-way cycle of crossover reactions proceeded via concurrent cationic vinyl-addition, ring-opening, and carbonyl-addition mechanisms. The stabilities of the resulting sequences and the propagation reactions were responsible for the occurrence of highly selective crossover reactions from the propagating chain ends derived from each monomer. In addition, the homopropagation reactions of IPVE and oxetane preferentially occurred over the crossover reactions to oxetane and MEK, respectively, resulting in the formation of multiblock polymers with repeating constitutional units of a poly(IPVE) block, a polyoxetane block, and one MEK unit. Detailed analysis of chain end structures by NMR revealed that mono- and difluorophosphates generated via the hydrolysis of PF_6^- contributed to the terpolymerization, which was partly mediated by long-lived species. The oxonium ion derived from oxetane also likely functioned as a long-lived species, as indicated by the incorporation of a quencher fragment into the chain end of the polymers. The strategy and initiating systems designed in this study will surely lead to the synthesis of polymers with controlled sequences, predetermined MWs, and various intriguing functions via the polymerization of different types of monomers.

Associated Content

Supporting Information: The Supporting Information is available free of charge on the ACS Publication website at DOI: 10.1021/acs.macromol.xxxxx. Polymerization data, ^{1}H, ^{13}C, ^{1}H–^{1}H COSY, ^{1}H–^{13}C HSQC, ^{1}H–^{13}C HMBC, ^{31}P and ^{19}F NMR spectra of product polymers, ^{31}P and ^{19}F NMR spectra of an initiator, and ESI-MS spectrum of a polymer.

Acknowledgments

This work was partially supported by JSPS KAKENHI grant numbers 26708014 and 16K14005.

References and Notes

1. Saegusa, T. Spontaneous Alternating Copolymerization via Zwitterion Intermediates. *Angew. Chem. Int. Ed. Engl.* **1977**, *16*, 826–835.
2. Saegusa, T. Sequence Regulation in Spontaneous Binary and Ternary Copolymerizations via Zwitterion Intermediates. *Makromol. Chem., Suppl.* **1981**, *4*, 73–84.
3. Okada, M.; Yamashita, Y.; Ishii, Y. Cationic Copolymerization of 1,3-Dioxolane with Styrene. *Makromol. Chem.* **1966**, *94*, 181–193.
4. Okada, M.; Yamashita, Y. Cationic Copolymerization of Cyclic Formals and Vinyl Ethers. *Makromol. Chem.* **1969**, *126*, 266–275.
5. Simionescu, C. I.; Grigoras, M.; Bicu, E.; Onofrei, G. Spontaneous Copolymerization of 2-Methyl-2-oxazoline and *N*-Phenyl Maleimide. *Polym. Bull.* **1985**, *14*, 79–83.
6. Rivas, B. L.; Pizarro, C.; Canessa, G. S. Copolymerization via Zwitterion 11. *N*-Phenylmaleimide with 2-Ethyl-2-oxazoline. *Polym. Bull.* **1988**, *19*, 123–128.
7. Hagiwara, T.; Takeda, M.; Hamana, H.; Narita, T. Copolymerization of *N*-Phenylmaleimide and Propylene Oxide Initiated with Organozinc Compounds. *Macromolecules* **1989**, *22*, 2025–2026.
8. Ikeda, Y.; Yoshida, Y.; Ishihara, K.; Hamana, H.; Narita, T.; Hagiwara, T. Copolymerization of 3,3,3-Trifluoro-1,2-epoxypropane with *N*-Phenylmaleimide Using Organozinc Initiators. *Macromol. Rapid Commun.* **1996**, *17*, 713–721.
9. Yang, H.; Xu, J.; Pispas, S.; Zhang, G. Hybrid Copolymerization of ε-Caprolactone and Methyl Methacrylate. *Macromolecules* **2012**, *45*, 3312–3317.
10. Kanazawa, A.; Kanaoka, S.; Aoshima, S. Rational Design of Oxirane Monomers for Efficient Crossover Reactions in Concurrent Cationic Vinyl-Addition and Ring-Opening Copolymerization with Vinyl Ethers. *Macromolecules* **2014**, *47*, 6635–6644.
11. Aoshima, H.; Uchiyama, M.; Satoh, K.; Kamigaito, M. Interconvertible Living Radical and Cationic Polymerization through Reversible Activation of Dormant Species with Dual Activity. *Angew. Chem.*

Int. Ed. **2014**, *53*, 10923–10936.

12. Hsieh, H. L. Terpolymerization of Cyclic Ethers with Cyclic Anhydride. *J. Macromol. Sci., Chem.* **1973**, *A7*, 1525–1535.
13. Saegusa, T.; Kobayashi, S.; Kimura, Y. Polymerization via Zwitterion. 12. Novel 1:1:1 Alternating Terpolymerizations of 2-Phenyl-1,3,2-dioxaphospholane, Electron Deficient Vinyl Monomers of Acrylonitrile and Acrylate, and Carbon Dioxide. *Macromolecules* **1977**, *10*, 68–72.
14. Kanazawa, A.; Aoshima, S. Exclusive One-Way Cycle Sequence Control in Cationic Terpolymerization of General-Purpose Monomers via Concurrent Vinyl-Addition, Ring-Opening, and Carbonyl-Addition Mechanisms. *ACS Macro Lett.* **2015**, *4*, 783–787.
15. Rose, J. B. Cationic Polymerisation of Oxacyclobutanes. Part I. *J. Chem. Soc.* **1956**, 542–546.
16. Rose, J. B. Cationic Polymerisation of Oxacyclobutanes. Part II. *J. Chem. Soc.* **1956**, 546–555.
17. Saegusa, T.; Hashimoto, Y.; Matsumoto, S. Ring-Opening Polymerization of Oxacyclobutane by Boron Trifluoride. Concentration of Propagating Species and Rate of Propagation. *Macromolecules* **1971**, *4*, 1–3.
18. Saegusa, T.; Fujii, H.; Kobayashi, S.; Ando, H.; Kawase, R. Kinetic Studies on Ring-Opening Polymerization of Unsubstituted, 3-Methyl-, and 3,3-Dimethyloxacyclobutanes by Boron Trifluoride Catalyst. Methyl-Substituent Effects on Rate of Propagation. *Macromolecules* **1973**, *6,* 26–32.
19. Dreyfuss, P.; Dreyfuss, M. P. The Formation of Cyclic Oligomers Accompanying the Polymerization of Oxetane. *Polym. J.* **1976**, *8*, 81–87.
20. Black, P. E.; Worsfold, D. J. The Polymerization of Oxetane with Hexafluorophosphate Salts. *Can. J. Chem.* **1976**, *54*, 3325–3329.
21. Bouchékif, H.; Philbin, M. I.; Colclough, E.; Amass, A. J. Cationic Ring-Opening Polymerization of Oxetane via a Non-Steady-State Controlled Polymerization Process: A Comparison of Initiators Yielding Living and Nonliving Polymers. *Macromolecules* **2008**, *41*, 1989–1995.
22. Kahveci, M. U.; Yagci, Y.; Avgeropoulos, A.; Tsitsilianis, C. In *Polymer Science: A Comprehensive Reference*; Matyjaszewski, K.; Möller, M., Eds.; Elsevier B.V.: Amsterdam, 2012; vol. *6.13*.
23. Hirao, A.; Goseki, R.; Ishizone, T. Advances in Living Anionic Polymerization: From Functional Monomers, Polymerization Systems, to Macromolecular Architectures. *Macromolecules* **2014**, *47*, 1883–1905.
24. Polymeropoulos, G.; Zapsas, G.; Ntetsikas, K.; Bilalis, P.; Gnanou, Y.; Hadjichristidis, N. 50th Anniversary Perspective: Polymers with Complex Architectures. *Macromolecules* **2017**, *50*, 1253–1290.
25. Kennedy, J. P.; Chou, R. T. Carbocationic Polymerization in the Presence of Sterically Hindered Bases. I. α-Methylstyrene Polymerization in the Presence of Sterically Hindered Bases. *J. Macromol. Sci., Chem.* **1982**, *A18*, 11–16.
26. Bae, Y.-C.; Faust, R. The Role of Pyridine Derivatives in Living Carbocationic Polymerization: Lewis

Base or Nucleophile? *Macromol. Symp.* **1998**, *132*, 11–23.

27. Storey, R. F.; Curry, C. L.; Hendry, L. K. Mechanistic Role of Lewis Bases and Other Additives in Quasiliving Carbocationic Polymerization of Isobutylene. *Macromolecules* **2001**, *34*, 5416–5432.
28. Kishimoto, Y.; Aoshima, S.; Higashimura, T. Living Cationic Polymerization of Vinyl Monomers by Organoaluminum Halides. 4. Polymerization of Isobutyl Vinyl Ether by $EtAlCl_2$ in the Presence of Ether Additives. *Macromolecules* **1989**, *22*, 3877–3882.
29. Aoshima, S.; Kanaoka, S. A Renaissance in Living Cationic Polymerization. *Chem. Rev.* **2009**, *109*, 5245–5287.
30. Saegusa, T.; Matsumoto, S. Determination of Concentration of Propagating Species in Cationic Polymerization of Tetrahydrofuran. *J. Polym. Sci.: Part A-1* **1968**, *6*, 1559–1565.
31. The average unit number of MEK was less than one because of the difference in the numbers of acetal moieties and MEK units per chain.
32. At a higher temperature of 30 °C, the homopolymerization of oxetane proceeded successfully.
33. Laurence, C.; Graton, J.; Berthelot, M.; Besseau, F.; Le Questel, J.-Y.; Luçon, M.; Ouvrard, C.; Planchat, A.; Renault, E. An Enthalpic Scale of Hydrogen-Bond Basicity. 4. Carbon π Bases, Oxygen Bases, and Miscellaneous Second-Row, Third-Row, and Fourth-Row Bases and a Survey of the 4-Fluorophenol Affinity Scale. *J. Org. Chem.* **2010**, *75*, 4105–4123.
34. Aoshima, S.; Fujisawa, T.; Kobayashi, E. Living Cationic Polymerization of Isobutyl Vinyl Ether by $EtAlCl_2$ in the Presence of Ether Additives: Cyclic Ethers, Cyclic Formals, and Acyclic Ethers with Oxyethylene Units. *J. Polym. Sci., Part A: Polym. Chem.* **1994**, *32*, 1719–1728.
35. Shaffer, T. D.; Ashbaugh, J. R. Noncoordinating Anions in Carbocationic Polymerization *J. Polym. Sci., Part A: Polym. Chem.* **1997**, *35*, 329–344.
36. Dreyfuss, M. P.; Westfahl, J. C.; Dreyfuss, P. The Reaction of Trityl Salts with 2-Methyltetrahydrofuran and with Tetrahydrofuran. *Macromolecules* **1968**, *1*, 437–441.
37. This method is based on the generation of carbocations from alkyl halides and $AgPF_6$ in past studies (references 38–40).
38. Dreyfuss, P.; Kennedy, J. P. Alkyl Halides in Conjunction with Inorganic Salt for the Initiation of the Polymerization and Graft Copolymerization of Heterocycles. *J. Polym. Sci.: Polym. Symp.* **1976**, *56*, 129–137.
39. Burgess, F. J.; Cunliffe, A. V.; Richards, D. H.; Thompson, D. Organic Halides as Cationic Initiators. *Polymer* **1978**, *19*, 334–340.
40. Uchiyama, M.; Satoh, K.; Kamigaito, M. Diversifing Cationic RAFT Polymerization with Various Counteranions: Generation of Cationic Species from Organic Halides and Various Metal Salts. *ACS Macro Lett.* **2016**, *5*, 1157–1161.
41. Habibi, M. H.; Mallouk, T. E. Photochemical Selective Fluorination of Organic Molecules Using Mercury (II) Fluoride. *J. Fluorine Chem.* **1991**, *51*, 291–294.

42. Wagner, R.; Korth, M.; Streipert, B.; Kasnatscheew, J.; Gallus, D. R.; Brox, S.; Amerller, M.; Cekic-Laskovic, I.; Winter, M. Impact of Selected $LiPF_6$ Hydrolysis Products on the High Voltage Stability of Lithium-Ion Battery Cells. *ACS Appl. Mater. Interfaces* **2016**, *8*, 30871–30878.
43. Wilken, S.; Treskow, M.; Scheers, J.; Johansson, P.; Jacobsson, P. Initial Stages of Thermal Decomposition of $LiPF_6$-Based Lithium Ion Battery Electrolytes by Detailed Raman and NMR Spectroscopy. *RSC Adv.* **2013**, *3*, 16359–16364.
44. Nowak, S.; Winter, M. Review—Chemical Analysis for a Better Understanding of Aging and Degradation Mechanisms of Non-Aqueous Electrolytes for Lithium Ion Batteries: Method Development, Application and Lessons Learned. *J. Electrochem. Soc.* **2015**, *162*, A2500–A2508.
45. Plakhotnyk, A. V.; Ernst, L.; Schmutzler, R. Hydrolysis in the System $LiPF_6$–Propylene Carbonate–Dimethyl Carbonate–H_2O. *J. Fluorine Chem.* **2005**, *126*, 27–31.
46. Vortmann, B.; Nowak, S.; Engelhard, C. Rapid Characterization of Lithium Ion Battery Electrolytes and Thermal Aging Products by Low-Temperature Plasma Ambient Ionization High-Resolution Mass Spectrometry. *Anal. Chem.* **2013**, *85*, 3433–3438.
47. Uchiyama, M.; Satoh, K.; Kamigaito, M. A Phosphonium Intermediate for Cationic RAFT Polymerization. *Polym. Chem.* **2016**, *7*, 1387–1396.
48. The chemical shifts of these peaks are consistent with the corresponding peaks of (3-vinyloxypropoxy)benzene (4.08ppm; reference 49) and [2-(2-chloroethoxy)ethoxy]benzene (4.11ppm; reference 50)
49. Ram, R. N.; Singh, V. Diazotisation of Aromatic Amines and Solvolysis of Diazonium Salts in Ethylene Glycol Ethers. *J. Chem. Res.* **2006**, 800–803.
50. Sugimura, T.; Yamasaki, A.; Okuyama, T. Stereocontrolled Intramolecular *meta*-Arene–Alkene Photocycloaddition Reactions Using Chiral Tethers: Efficiency of the Tether Derived from 2,4-Pentanediol. *Tetrahedron: Asymmetry* **2005**, *16*, 675–683.

TOC Graphic

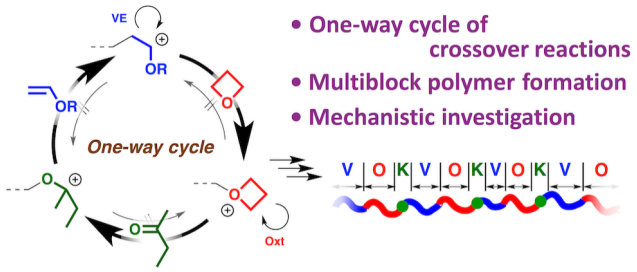

Cationic Terpolymerization of Vinyl Ether, Oxetane, and Ketone via the Concurrent Vinyl-Addition, Ring-Opening, and Carbonyl-Addition Mechanisms: Multiblock Polymer Synthesis and Mechanistic Investigation

Arihiro Kanazawa and Sadahito Aoshima**